Journal of Colloid and Interface Science 452 (2015) 126–133

Contents lists available at ScienceDirect

Journal of Colloid and Interface Science

www.elsevier.com/locate/jcis

ZnO/Ag/CdO nanocomposite for visible light-induced photocatalytic degradation of industrial textile effluents

R. Saravanan [a,f,*], M. Mansoob Khan [b], Vinod Kumar Gupta [c,d,e], E. Mosquera [f], F. Gracia [a], V. Narayanan [g], A. Stephen [h,*]

[a] Department of Chemical Engineering and Biotechnology, University of Chile, Beauchef 850, Santiago, Chile
[b] School of Chemical Engineering, Yeungnam University, Gyeongsan-si, Gyeongbuk 712-749, South Korea
[c] Department of Chemistry, Indian Institute of Technology Roorkee, Roorkee 247 667, India
[d] Center for Environment and Water, The Research Institute, King Fahd University of Petroleum and Minerals, Dhahran, Saudi Arabia
[e] Department of Applied Chemistry, University of Johannesburg, Johannesburg, South Africa
[f] Nanoscale Materials Laboratory, Department of Materials Science, University of Chile, Avenida Tupper 2069, Santiago, Chile
[g] Department of Inorganic Chemistry, University of Madras, Guindy Campus, Chennai 600 025, India
[h] Department of Nuclear Physics, University of Madras, Guindy Campus, Chennai 600 025, India

GRAPHICAL ABSTRACT

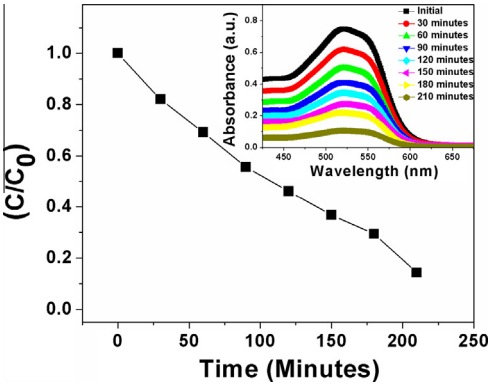

ARTICLE INFO

Article history:
Received 30 January 2015
Accepted 17 April 2015
Available online 23 April 2015

Keywords:
Nanocomposite
ZnO/Ag/CdO
Visible light
Industrial textile effluent
Photocatalysis

ABSTRACT

A ternary ZnO/Ag/CdO nanocomposite was synthesized using thermal decomposition method. The resulting nanocomposite was characterized by X-ray diffraction, field emission scanning electron microscopy, transmission electron microscopy, UV–Vis spectroscopy, and X-ray photoelectron spectroscopy. The ZnO/Ag/CdO nanocomposite exhibited enhanced photocatalytic activity under visible light irradiation for the degradation of methyl orange and methylene blue compared with binary ZnO/Ag and ZnO/CdO nanocomposites. The ZnO/Ag/CdO nanocomposite was also used for the degradation of the industrial textile effluent (real sample analysis) and degraded more than 90% in 210 min under visible light irradiation. The small size, high surface area and synergistic effect in the ZnO/Ag/CdO nanocomposite is responsible for high photocatalytic activity. These results also showed that the Ag nanoparticles induced visible light activity and facilitated efficient charge separation in the ZnO/Ag/CdO nanocomposite, thereby improving the photocatalytic performance.

* Corresponding authors at: Department of Chemical Engineering and Biotechnology, Faculty of Mathematics and Physical Sciences, University of Chile, Beauchef 850, Santiago, Chile. Fax: +56 2 699 1084 (R. Saravanan).
E-mail addresses: saravanan3.raj@gmail.com (R. Saravanan), Stephen_arum@hotmail.com (A. Stephen).

http://dx.doi.org/10.1016/j.jcis.2015.04.035
0021-9797/

1. Introduction

Water contamination has led the major health risks round the globe which is growing at a faster rate every year [1]. United Nations has reported that worldwide about 1800 children under the age of five years dies every day from diarrhoea which occurs due to contaminated water [1]. The increase in the use of organic pollutants in various industries nowadays causing several harmful effects to humans as well as ecological systems. The waste water from the industries is directly released into the water bodies, thus contaminating the entire fresh water resources. Wastewater treatment and recycling is an important concern and the researchers are looking forward for inexpensive and suitable technologies. Numerous technologies have been developed to sustain green atmosphere [2–4]. Among them heterogeneous catalytic processes has paid more attention for the treatment of waste water. This is one of the green technologies that offer great potential for complete elimination of toxic chemicals from the environment because of its high efficiency and broad applicability. Even under mild conditions of temperature and pressure almost complete degradation of pollutants can be achieved. The most significant feature of this process is its cost-effectiveness [5–10].

In this study zinc oxide has been chosen because of its intriguing properties such as non-toxicity, higher photocatalytic efficiency, good sensing behaviour and other versatile applications [11]. However, the main disadvantage of ZnO is that it is active under UV light, hence, low activity in solar spectrum. Therefore, various efforts have been made to increase the ZnO activity in visible light and hence their higher degradation rate of pollutants [11]. The enhancement of photocatalytic activity of ZnO mainly depends on the prevention of electron–hole recombination process. The hindering of electron–hole recombination is achieved through doping with a metal (Ag, Cd, Cu, Co, Fe, or Mn) or a non-metal (N, S, or F) in ZnO or developing ZnO based composites such as ZnO/metal, ZnO/metal oxide and ZnO/polymer [12–18].

Saravanan et al. reported that the modification of ZnO with CdO (95:5 weight ratios) effectively shifted the photocatalytic activity from UV to visible light [19]. The ZnO/CdO composite system revealed that the degradation of methylene blue under visible light irradiation for 6 h was achieved because of the retardation of back reaction between CdO and ZnO which produces more number of charge carriers which would increase the degradation efficiency. Thus, the efficiency of photogenerated electron–hole in ZnO/CdO could be higher than those of pure ZnO [19]. In contrast to this, different weight percentage of silver (Ag) coupled with ZnO system showed better photocatalytic activity under visible light due to their lower band gap energy and also the system prevents the fast electron–hole recombination [11,20]. The size, surface area and the amount of Ag were the major factors that affected the photocatalytic activities of ZnO. In particular, ZnO/Ag (90:10) system has showed higher photocatalytic activity compared with other weight percentages and it was successfully used for the degradation of textile dyes for 4 h visible light irradiation [20].

The main aim of this study is to synthesize a novel ternary ZnO/Ag/CdO photocatalyst with improved photodegradation efficiency in a short interval of visible light irradiation. The present work focuses on the synthesis and catalytic activity of the ZnO/Ag/CdO nanocomposite which was prepared in the ratio of (80:10:10) using thermal decomposition method. The prepared catalysts were characterized by different techniques and used for the photocatalytic degradation of methylene blue, methyl orange and effluents from the textile industries (real sample analysis) under visible light irradiation.

2. Experimental

2.1. Materials

For the synthesis of photocatalyst, the required chemicals such as zinc acetate dihydrate, silver acetate, and cadmium acetate were purchased from Sigma–Aldrich. Methyl orange (MO) and methylene blue (MB) were procured from Rankem Chemicals, India, and used without further purification. All the aqueous solutions were prepared using double distilled water.

2.2. Methods

The phases of the synthesized materials were identified by X-ray diffractometer (Rich Seifert 3000, Germany) using Cu $K\alpha_1$ radiation with λ = 1.5406 Å. Transmission electron microscopy analysis was carried out using microscope (TEM, Mark II, JEOL 2000FX, Tokyo, Japan), operated at 200 kV. Chemical states of catalysts were examined using X-ray photoelectron spectroscopy (XPS, DRA 400 – XM1000 OMICRON, ESCA$^+$, Omicron Nanotechnology, Germany). The Brunauer–Emmett–Teller (BET, Micromeritics ASAP 2020, USA) was used to calculate the specific surface area. Surface morphology, elemental analysis and energy dispersive X-ray spectroscopy (EDS) analysis was carried out using field emission scanning electron microscope (FE-SEM, HITACHI-SU6600, Hitachi, Japan). The optical band gap and photocatalytic activity was measured by UV–Vis spectrophotometer (RX1, Perkin – Elmer, USA). Degradation of textile effluents were confirmed by total organic carbon content (TOC) which was carried out using (Shimadzu TOC analyser, Japan) TOC analyser and chemical oxygen demand (COD) was measured using (SPECTRA LAB, India) COD DIGESTER 2015 M.

2.3. Synthesis of different catalysts

In this work, pure ZnO, Ag, and CdO nanoparticles, and ZnO/Ag and ZnO/CdO nanocomposites were synthesized using methods reported elsewhere [19,20]. Similarly, ZnO/Ag/CdO nanocomposite was synthesized using zinc acetate dihydrate, silver acetate and cadmium acetate (80:10:10) which were mixed without any additive which was later grounded well for 3 h. Finally the grounded powder was taken into alumina crucible and covered with a lid and calcined at 350 °C for 3 h in a muffle furnace. During this process, the temperature was raised at a uniform rate of 4 °C/min. After the heat treatment, the sample was naturally cooled to room temperature. The preparation mechanism is similar to vapour to solid mechanism [21]. The high temperature generated oxide vapour from raw material which settled or deposited when the temperature was lowered. Pan et al. [21] reported that surface defects or dislocations of the substrate (crucible) provide promising nucleation sites for the oxide vapour, similarly, in the present work; the crucible provides such nucleation sites [21]. The vapour condenses on these sites, forming seeds for a continuous deposition of oxide vapour. Noble metal nanoparticles can be obtained directly using thermal decomposition method in the presence of air [22]. In this synthesis silver (Ag) nanoparticles were prepared using the same method.

2.4. Photocatalytic experiments

The visible light irradiation was carried out using a projection lamp (7748XHP, 250W, Philips) in a photo-reactor. The 600 mL cylindrical photo-reactor was covered by 0.5% aqueous $K_2Cr_2O_7$ solution circulated in the glass jacket which was used for the purpose of UV cut-off. The preparation of water soluble model dyes

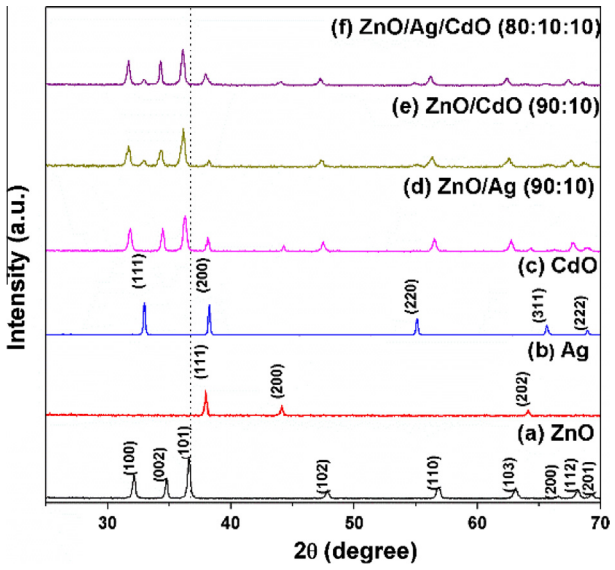

Fig. 1. The XRD patterns of the synthesized (a) pure ZnO, (b) Ag, (c) CdO, (d) ZnO/Ag, (e) ZnO/CdO, and (f) ZnO/Ag/CdO catalysts.

such as MB and MO were made as reported earlier [19,20]. The synthesized materials ZnO, ZnO/Ag, ZnO/CdO and ZnO/Ag/CdO were used for the photocatalytic degradation of MO and MB as previously reported [19,20]. The initial and irradiated methylene blue and methyl orange concentration of solutions were examined by UV–Vis spectrophotometer at a wavelength of 664 and 464 nm respectively.

The optimized higher degradation ternary photocatalyst (ZnO/Ag/CdO) was further used to study the photocatalytic degradation of industrial textile effluents (real sample analysis) which was collected from the textile industry (Tirupur, Tamilnadu, India). Before performing the photocatalytic degradation experiment, 50 mL of the textile effluent was diluted with 450 mL of distilled water (1:9 ratio) in order to reduce its turbidity property. So that, light can pass through the entire suspension without any loss. The initial and irradiated textile effluents concentrations were examined by UV–Vis spectrophotometer at a wavelength of 520 nm respectively.

3. Results and discussion

The phase and structure of the synthesized materials were confirmed through XRD analysis. Fig. 1a exhibits (100), (002), (101), (102), (110), (103), (200), (112) and (201) characteristic planes indicating hexagonal structure for ZnO. The lattice parameters for pure ZnO sample matches well with the JCPDS file no: 79-0208. The XRD pattern for Ag is shown in Fig. 1b and the obtained characteristic planes (111), (200) and (202) were indexed to be of cubic structure. The lattice parameters were similar to JCPDS file no: 89-3722. The diffraction pattern for the CdO sample is depicted in Fig. 1c. The planes (111), (200), (220), (311) and (203) indicate the cubic structure for CdO which coincides with the JCPDS No: 73-2245. The XRD pattern of binary material ZnO/Ag (90:10) was shown in Fig. 1d. This indicates the formation of metallic silver along with ZnO. On the other hand, the XRD pattern of ZnO/CdO (99:10) is shown by Fig. 1e. This pattern revealed the cubic structure for CdO and hexagonal structure for ZnO. Fig. 1f represents the XRD pattern for ternary (ZnO/Ag/CdO) system. All the diffraction peaks are exactly indexed and the peaks show the hexagonal structure for ZnO (JCPDS No: 79-0208), cubic structure for Ag (JCPDS No: 89-3722) and a cubic structure for CdO (JCPDS No. 73-2245).

Fig. 1(d–f) shows the XRD patterns for the binary (ZnO/CdO, ZnO/Ag) and ternary (ZnO/Ag/CdO) nanocomposites. In both the cases, it was observed that the peaks were shifted towards lower angle compared to the peaks of pure ZnO which is mark by dotted line. The lower shift in the peaks was due to the larger ionic radius of cadmium and silver compared to that of the smaller ionic radius of zinc. This observation is similar to the report of Ziabari et al. [23]. However, the addition of impurity (cadmium and silver) does not affect the structure of ZnO. The binary and ternary nanocomposites shows broad peaks which obviously indicate the sizes of the nanocomposite materials are small, whereas the pure material (ZnO, Ag and CdO) shows sharp peaks because of big size compared to the ZnO/Ag/CdO nanocomposite.

It is well known that when size of the catalyst will decrease, the surface area will be increased, the same trend has been observed in this work, which is confirmed by BET analysis as shown in Table 1. The ternary ZnO/Ag/CdO nanocomposite shows highest surface area (Table 1) compared with binary nanocomposites (ZnO/Ag and ZnO/CdO) and pure ZnO. The difference in their surface area was due to the synergetic effect among the components such as ZnO, Ag and CdO in the composite system [24,25]. The increase in the surface area was significant, hence, the larger surface area of ZnO/Ag/CdO nanocomposite will benefit the spatial separation of redox sites in the crystals which can enhance electron-transfer properties of the nanocomposite [26–28].

The FE-SEM images of pure ZnO, ZnO/Ag, ZnO/CdO and ZnO/Ag/CdO samples are shown in Fig. 2. FE-SEM images show the randomly distributed nanorods of uniform sizes and diameter. When compared with pure ZnO, and binary (ZnO/Ag and ZnO/CdO), ternary (ZnO/Ag/CdO) systems show nanorods along with spherical shape particle. It is evidently observed that the size of the nanorods decreases in the ternary nanocomposite system because of heterogeneous nucleation effect [29,30]. The addition of silver and cadmium oxide may influence the size and morphology of ZnO. Compared with binary and pure system, the ternary nanocomposite nanorods are smaller in size due to the nucleation and synergetic effect which is in accordance with the XRD and BET results. The presences of elements in the prepared samples were analyzed and confirmed using energy dispersive spectroscopy (EDS) and are shown by Fig. S1. The results of EDS spectra shows the presence of Zn and O in pure ZnO; Zn, O and Ag in ZnO/Ag; Zn, O and Cd in ZnO/CdO; and Zn, O, Ag, and Cd in ZnO/Ag/CdO. No any other impurities were observed. This further confirms the synthesis of the materials.

In addition, the shape and structure of the ZnO/Ag/CdO nanocomposite was also confirmed by TEM. The TEM image

Table 1
Surface area, optical band gap, degradation efficiency and first order rate constant of the synthesized catalysts.

Catalysts	Surface area BET (m^2/g)	Band gap (eV)	MB degradation efficiency 90 min (%)	Rate constant (k) for MB 10^{-4} min^{-1}	MO degradation efficiency 90 min (%)	Rate constant (k) for MO 10^{-4} min^{-1}
ZnO	8.7	3.22	4.9	0.085	6.1	0.065
ZnO/Ag (90:10)	14.1	2.86	91.1	3.666	82.3	1.111
ZnO/CdO (90:10)	13.2	2.90	49.7	0.777	49.1	0.715
ZnO/Ag/CdO (80:10:10)	21.5	2.63	98.3	5.666	97.8	4.322

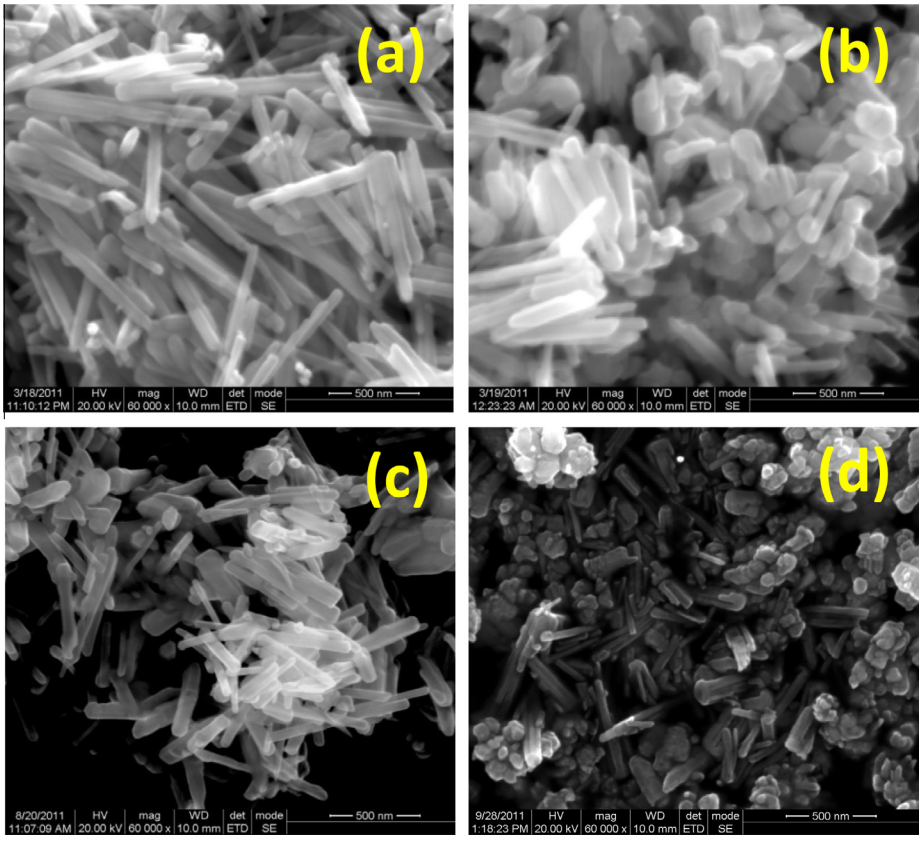

Fig. 2. The FE-SEM images of (a) pure ZnO, (b) ZnO/Ag, (c) ZnO/CdO, and (d) ZnO/Ag/CdO.

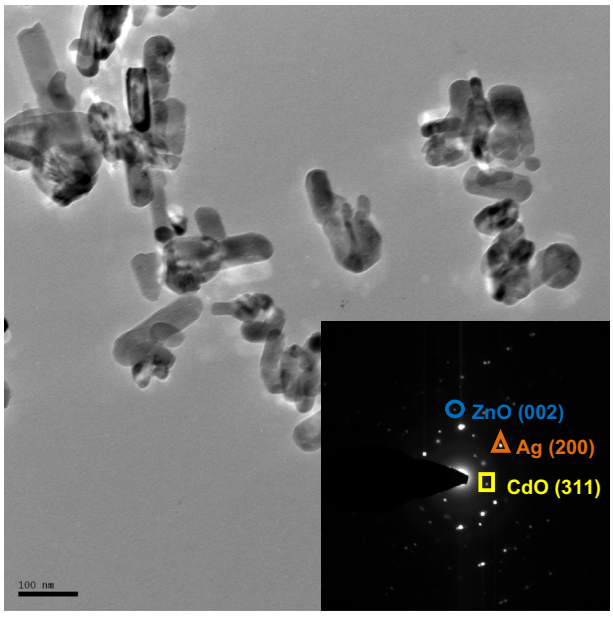

Fig. 3. TEM image (inset, SAED) of ZnO/Ag/CdO nanocomposite.

(Fig. 3) of ZnO/Ag/CdO nanocomposite is in agreement with the results of FE-SEM, which also showed nanorods along with closely attached spherical shaped nanoparticles. The SAED pattern (inset of Fig. 3) of the ternary nanocomposite clearly reveals that the (002) plane matched with a hexagonal structure of ZnO (JCPDS No: 79-0208), (200) plane confirmed the cubic structure of Ag nanoparticles (JCPDS No: 89-3722) whereas (311) plane confirmed the cubic structure of CdO (JCPDS No: 73-2245). The SAED pattern further confirms the synthesis of the ZnO/Ag/CdO nanocomposite which is concomitant with the XRD results.

The presence of elements and their oxidation states on the surface of the ZnO/Ag/CdO nanocomposite was confirmed by XPS analysis. Fig. 4a shows the XPS survey spectrum of ZnO/Ag/CdO (80:10:10) nanocomposite which confirms the presence of the Zn, Cd, Ag, O and C. Fig. 4(b–d) exhibit the high resolution XPS spectra of Zn 2p, Ag 3d and Cd 3d respectively. As shown in Fig. 4b, Zn $2p_{3/2}$ and Zn $2p_{1/2}$ states at the binding energies of 1021.7 eV and 1045.1 eV respectively which confirms the 2 + oxidation state of zinc, which is consistent with the previous reports [18,31,32]. Fig. 4c shows the binding energies for Ag 3d at 367.5 eV and 373.5 eV which represents the Ag $3d_{5/2}$ and Ag $3d_{3/2}$ peaks [33]. Fig. 4d shows the XPS spectrum of Cd corresponding the binding energies of 406.2 eV and 413.1 eV for Cd $3d_{5/2}$ and Cd $3d_{3/2}$ peaks of Cd (II) states which is similar to the previous reports [16,31,32]. Fig. 4e shows the deconvoluted O 1s spectrum indicating three types of oxygen were present having the binding energies at 529.1 eV, 530.4 eV and 531.3 eV which were associated with ZnO, CdO and the surface hydroxyl group respectively [34]. Hence, XPS studies confirmed the oxidation states of the each element in the ZnO/Ag/CdO nanocomposite without any other impurity.

The optical band gaps of the synthesized catalysts were examined using UV–Vis absorption spectroscopy. Fig. 5 shows the absorption edges of the pure ZnO and binary (ZnO/Ag and ZnO/CdO) nanocomposites which lies between 350 and 400 nm. The absorption bands of the ternary (ZnO/Ag/CdO) catalysts are wider (400–600 nm) and it clearly indicates that ZnO/Ag/CdO nanocomposite showing absorption which is red shifted compared with pure ZnO which lies in the blue region of the spectrum. It is clearly

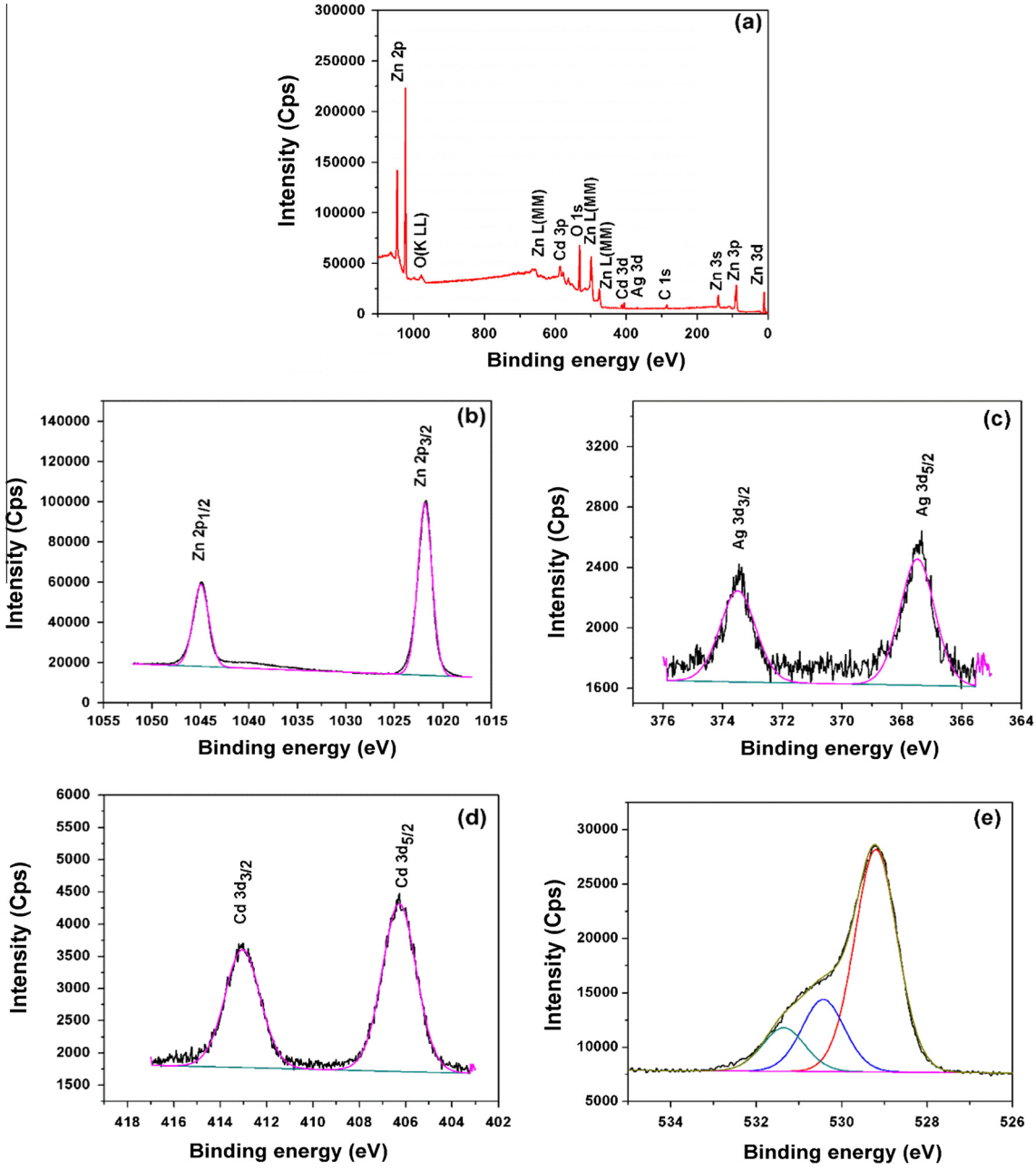

Fig. 4. The XPS spectra of ZnO/Ag/CdO nanocomposite (a) survey, (b) zinc, (c) silver, (d) cadmium, and (e) oxygen.

observed that the ZnO absorption edge is ~360 nm and the corresponding wavelength exists in the UV region. The band gap energies were calculated based on Tauc's plot (Fig. S2) and the values are represented in Table 1. The band gap of the ternary system reduces as compared with the binary and pure ZnO. The variation of band gap arises because of the synergetic effect. The comparable statement has been stated in previous literature [35,36]. Wang et al. reported the bandgap value of coupled oxide (ZnO/SnO_2) which is lower than that of pure ZnO because of its synergistic effect. The bandgap value of SnO_2 is 2.6 eV which may be the reason that the band gap energy decreases when the ZnO particles are coupled with SnO_2 powders [36]. Similar phenomenon could be arising in the ternary ZnO/Ag/CdO nanocomposite system. ZnO band gap value is high as compared with cadmium and surface phonon resonance value of silver. Hence, the UV–Vis absorption results indicated that the prepared ternary and binary catalysts have absorption bands in the visible region. It is also well known that the photocatalytic process mainly depends on the wavelength of irradiated light. Therefore, the photocatalytic process by the ternary nanocomposites could be better than binary nanaocomposites under visible light irradiation.

3.1. Photocatalytic degradation

The photocatalytic activity of ZnO, ZnO/Ag, ZnO/CdO and ZnO/Ag/CdO photocatalysts were tested to degrade the model organic dyes such as MB and MO under visible light irradiation. Time course degradation curves for MB and MO were shown in Fig. 6(a and b) respectively. The concentration of MB and MO has been decreased with increasing visible light irradiation time which confirms that the photodegradation of model dyes has taken place in the presence of ZnO/Ag/CdO photocatalyst. In comparison to

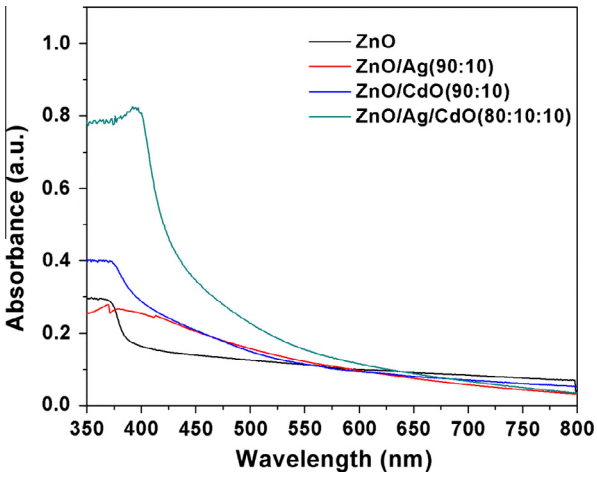

Fig. 5. UV–Vis absorption spectra of the prepared catalysts.

degradation of MO, degradation rate of MB was much faster because of its simple structure. Also methylene blue acts as sensitizer of the photocatalyst [37]. From Fig. 6, it is observed that there is very less decolouration by the pure ZnO due to its larger band gap. Among the prepared samples, ZnO/Ag/CdO shows higher degradation efficiency (Table 1) within a short irradiation time. In our previous report, ZnO/CdO (95:5) composite showed the degradation of MB under visible light irradiation for 6 h [19]. The observed photocatalytic activity was in the order of ZnO/Ag/CdO > ZnO/Ag > ZnO/CdO > ZnO.

The first order rate constant (k) of the photocatalytic reaction was calculated from the following equation $k = \ln(C/Co)/t$, where Co and C are the concentrations of model dyes at the irradiation time 0 and t min. Fig. S3(a) and (b) represent linear plots of $\ln(C/Co)$ with respective irradiation time. Based on the slope of the liner fitted graph, the calculated k values (Table 1) shows that the ZnO/Ag/CdO nanocomposite has high reaction rate than pure ZnO, ZnO/Ag, and ZnO/CdO. Furthermore, as the ZnO/Ag/CdO nanocomposite shows higher photocatalytic activity for the degradation of MO and MB under visible light irradiation, therefore, it was employed for the photocatalytic degradation of industrial textile effluent (real sample analysis) under visible light irradiation.

Fig. 7 shows the changes in absorption of the degraded industrial textile effluent solution with time in presence of ZnO/Ag/CdO nanocomposite under visible light irradiation. The decrease in the C/Co value with increase in irradiation time was evidently shown in Fig. 7. It was found that more than 90% of the degradation of the industrial textile effluent was achieved within 210 min using ZnO/Ag/CdO nanocomposite as a photocatalyst under visible light irradiation. The degradation of coloured pollutants in waste water is often more significant than the degradation of other organic colourless pollutants because of their higher toxicity [38]. The ZnO/Ag/CdO nanocomposite removes the colour of textile effluent, but still the complete removal of toxic components and mineralization needs to be further confirmed. Mineralization refers to the process where the harmful organic substances are converted into the harmless inorganic substance. During the photocatalytic process, sometimes the final degraded products are more toxic than the parent compounds. Hence, the mineralization and the toxic-free of the treated effluents are important while discharging back the treated water into the ecosystem. Hence, mineralization of industrial textile effluents was confirmed through TOC and COD experiments.

Fig. 8 shows the normalized TOC and COD results for the degradation of industrial textile effluents for different intervals of time. These results exhibited that the concentration of pollutants in industrial textile effluents decreases significantly with increasing visible light irradiation. The ZnO/Ag/CdO nanocomposite exhibits high photocatalytic activity not only in the decolourization but also by the effectively mineralization of colourless organic pollutants. The TOC and COD results represents that more than 90% of the initial industrial textile effluents were degraded and mineralized using ternary ZnO/Ag/CdO nanocomposite as a photocatalyst.

3.2. Photocatalytic pathways

The ternary ZnO/Ag/CdO nanocomposite shows higher degradation efficiency by photocatalytic degradation of MB, MO and industrial textile effluent within short interval of irradiation time. The enhanced visible light photocatalytic activity of this system possibly depends on the following reasons:

The photocatalytic activity mainly depends on the size, morphology and surface area of the catalyst. The weight ratios of the ternary ZnO/Ag/CdO nanocomposite system (80:10:10) in the present work is based on the higher degradation achieved in comparison to those of the binary nanocomposites. The particle size of the synthesized ternary nanocomposite was small compared with binary and pure ZnO systems which were evidently confirmed by TEM and FE-SEM. The smaller size of the ZnO/Ag/CdO nanocomposite gives high surface to volume ratio and can also create the possibility of indirect electron transition which in turn generates more number of electrons and holes. In other words, it is known that the photocatalytic redox reaction mainly takes place on the surface of the photocatalysts and the improved surface properties significantly influence the efficiency of the catalysts [26–28].

Another reason for the enhancement in the visible light-induced photocatalytic activity of the ZnO/Ag/CdO nanocomposite

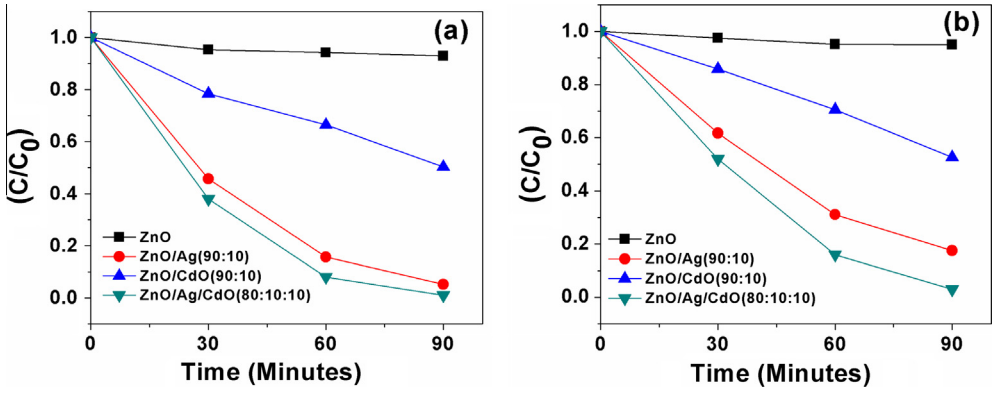

Fig. 6. Photocatalytic degradation time course curves for (a) MB and (b) MO.

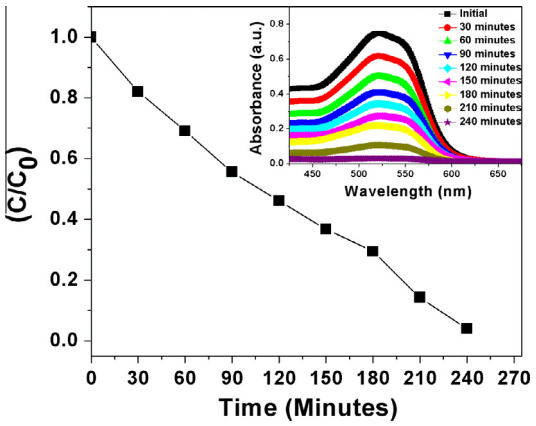

Fig. 7. Photocatalytic degradation of the industrial textile effluent using ZnO/Ag/CdO photocatalyst (inset, corresponding UV–Vis absorption band) under visible light irradiation.

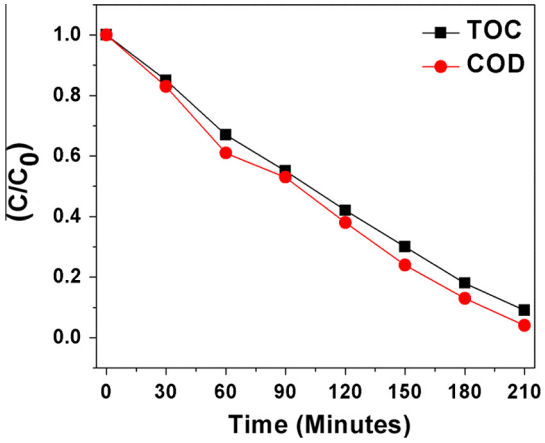

Fig. 8. TOC and COD plots showing the complete degradation and mineralization of the industrial textile effluent by ZnO/Ag/CdO nanocomposite under visible light irradiation.

system is that the ternary nanocomposite contains metallic Ag which has strong electron accepting ability and shows surface plasmon resonance phenomena [11,20]. As the Ag nanoparticles acts as electron traps, facilitating the electron–hole separation and subsequent transfer of the trapped electrons to the adsorbed O_2 which acts as an electron acceptor on the surface of ZnO and CdO. Also, the ternary nanocomposite having more than one pathway for the formation of electron–hole pair because of the three different interfaces and the electron–hole pair recombination is prevented to the maximum extent in the ternary nanocomposite [11,26,36,38–54]. As a result, the ternary photocatalyst ZnO/Ag/CdO exhibits the highest photocatalytic activity when compared to the binary photocatalysts (ZnO/Ag and ZnO/CdO) and pure ZnO.

4. Conclusions

This paper reports the synthesis of ternary ZnO/Ag/CdO nanocomposite using thermal decomposition method and effectively used as visible light-induced photocatalyst. The as-synthesized ZnO/Ag/CdO nanocomposite showed better photo catalytic degradation of MB, MO and industrial textile effluent under visible light irradiation in comparison to the binary ZnO/Ag and Zn/CdO nanocomposites. The small size, high surface area and synergistic effect within the ZnO/Ag/CdO nanocomposite seems responsible for the high visible light-induced photocatalysis.

Acknowledgments

We acknowledge National Centre for Nanoscience and Nanotechnology, University of Madras, Chennai, India for XPS and TEM characterizations. The authors (R.S., F.G.) acknowledge the support of CONICYT through the project CONICYT/FONDAP/15110019 and the postdoctoral fellowship granted to R.S.

Appendix A. Supplementary material

Supplementary data associated with this article can be found, in the online version, at http://dx.doi.org/10.1016/j.jcis.2015.04.035.

References

[1] Investing in water and sanitation: increasing access, reducing inequalities UN-water global analysis and assessment of sanitation and drinking-water GLASS, 2014.
[2] M.M. Khan, S.A. Ansari, D. Pradhan, M.O. Ansari, D.H. Han, J. Lee, M.H. Cho, J. Mater. Chem. A 2 (2014) 637–644.
[3] V.K. Gupta, I. Ali, T.A. Saleh, A. Nayak, S. Agarwal, RSC Adv. 2 (2012) 6380–6388.
[4] M.M. Khan, S.A. Ansari, M.I. Amal, J. Lee, M.H. Cho, Nanoscale 5 (2013) 4427–4435.
[5] A. Fujishima, K. Honda, Nature 238 (1972) 37–38.
[6] M.M. Khan, S.A. Ansari, M.O. Ansari, B.K. Min, J. Lee, M.H. Cho, J. Phys. Chem. C 118 (2014) 9477–9484.
[7] A. Fujishima, Tata N. Rao, Donald A. Tryk, J. Photochem. Photobio. C: Photochem. Rev. 1 (2000) 1–21.
[8] M.M. Khan, S.A. Ansari, D. Pradhan, D.H. Han, J. Lee, M.H. Cho, Ind. Eng. Chem. Res. 53 (2014) 9754–9763.
[9] M.M. Khan, J. Lee, M.H. Cho, J. Ind. Eng. Chem. 20 (2014) 1584–1590.
[10] M.M. Khan, S.A. Ansari, J.H. Lee, M.O. Ansari, J. Lee, M.H. Cho, J. Colloid Interface Sci. 431 (2014) 255–263.
[11] S.A. Ansari, M.M. Khan, M.O. Ansari, J. Lee, M.H. Cho, J. Phys. Chem. C 117 (2013) 27023–27030.
[12] R. Ullah, J. Dutta, J. Hazard. Mater. 156 (2008) 194–200.
[13] Z. Han, L. Ren, Z. Cui, C. Chen, H. Pan, J. Chen, Appl. Catal. B: Environ. 126 (2012) 298–305.
[14] Y. Jiang, Y. Sun, H. Liu, F. Zhu, H. Yin, Dyes Pigm. 78 (2008) 77–83.
[15] S.S. Shinde, C.H. Bhosale, K.Y. Rajpure, J. Photochem. Photobiol. B: Biol. 113 (2012) 70–77.
[16] R. Qiu, D. Zhang, Y. Mo, L. Song, E. Brewer, X. Huang, Y. Xiong, J. Hazard. Mater. 156 (2008) 80–85.
[17] Q. Yu, J. Li, H. Li, Q. Wang, S. Cheng, L. Li, Chem. Phys. Lett. 539 (2012) 74–78.
[18] S. Anandan, N. Ohashi, M. Miyauchi, Appl. Catal. B: Environ. 100 (2010) 502–509.
[19] R. Saravanan, H. Shankar, T. Prakash, V. Narayanan, A. Stephen, Mater. Chem. Phys. 125 (2011) 277–280.
[20] R. Saravanan, N. Karthikeyan, V.K. Gupta, P. Thangadurai, V. Narayanan, A. Stephen, Mater. Sci. Eng., C 33 (2013) 2235–2244.
[21] Z.W. Pan, Z.R. Dai, Z.L. Wang, Science 291 (2001) 1947–1949.
[22] V. Logvinenko, O. Polunina, Yu. Mikhailov, K. Mikhailov, B. Bokhonov, J. Therm. Anal. Cal. 90 (2007) 813–816.
[23] A.A. Ziabari, F.E. Ghodsi, J. Alloys Comp. 509 (2011). 8748–8875.
[24] Y. Li, H. Zhang, Z. Guo, J. Han, X. Zhao, Q. Zhao, S.J. Kim, Langmuir 24 (2008) 8351–8357.
[25] G. Tian, K. Pan, H. Fu, L. Jing, W. Zhou, J. Hazard. Mater. 166 (2009) 939–944.
[26] X. Yang, Y. Wang, L. Xu, X. Yu, Y. Guo, J. Phys. Chem. C 112 (2008) 11481–11489.
[27] J.M. Hermann, J. Disdier, P.J. Pichat, Phys. Chem. 90 (1986) 6028–6034.
[28] A. Sclafani, J.M. Hermann, J. Photochem. Photobiol., A 113 (1998) 181–188.
[29] T. He, Z. Zhou, W. Xu, Y. Cao, Z. Shi, W.P. Pan, Compos. Sci. Technol. 70 (2010) 1469–1475.
[30] K. Jayanthi, S. Chawla, K.N. Sood, M. Chhibara, S. Singh, Appl. Surf. Sci. 255 (2009) 5869–5875.
[31] A. Yousef, N.A.M. Barakat, T. Amna, A.R. Unnithan, S.S. Al-Deyab, H.Y. Kim, J. Lumin. 132 (2012) 1668–1677.
[32] R.M. Navarro, F. del Valle, J.L.G. Fierro, Int. J. Hydrogen Energy 33 (2008) 4265–4273.
[33] Y. Zheng, L. Zheng, Y. Zhan, X. Lin, Q. Zheng, K. Wei, Inorg. Chem. 46 (2007) 6980–6986.
[34] J. Mu, C. Shao, Z. Guo, Z. Zhang, M. Zhang, P. Zhang, B. Chen, Y. Liu, Appl. Mater. Interfaces 3 (2011) 590–596.
[35] M. Agrawal, S. Gupta, A. Pich, N.E. Zafeiropoulos, M. Stamm, Chem. Mater. 21 (2009) 5343–5348.
[36] H. Wang, S. Baek, J. Lee, S. Lim, Chem. Eng. J. 146 (2009) 355–361.

[37] R. Saravanan, E. Thirumal, V.K. Gupta, V. Narayanan, A. Stephen, J. Mol. Liq. 177 (2013) 394–401.
[38] G. Chen, L. Lei, P.L. Yue, Ind. Eng. Chem. Res. 38 (1999) 1837–1843.
[39] H.M. Sung-suh, J.R. Choi, H.J. Hah, S.M. Koo, Y.C. Ba, J. Photochem. Photobiol. A: Chem. 163 (2004) 37–44.
[40] L. Ge, M. Xu, H. Fang, J. Mol. Catal. A: Chem. 258 (2006) 68–76.
[41] Vinod K. Gupta, Rajeev Jain, Alok Mittal, Shilpi Agarwal, Shalini Sikarwar, Mater. Sci. Eng.: C 32 (2012) 12–17.
[42] T.A. Saleh, V.K. Gupta, Environ. Sci. Pollut. Res. 19 (2012) 1224–1228.
[43] V.K. Gupta, S.K. Srivastava, D. Mohan, S. Sharma, Waste Manage. 17 (1998) 517–522.
[44] V.K. Gupta, Alok Mittal, Jyoti Mittal, J. Colloid Interface Sci. 342 (2010) 518–527.
[45] V.K. Gupta, Alok Mittal, Dipika Kaur, Arti Malviya, Jyoti Mittal, J. Colloid Interface Sci. 337 (2009) 345–354.
[46] Alok Mittal, Arti Malviya, Jyoti Mittal, V.K. Gupta, J. Colloid Interface Sci. 340 (2009) 16–26.
[47] V.K. Gupta, Shilpi Agarwal, Tawfik A. Saleh, J. Hazardous Mat. 185 (2011) 17–23.
[48] V.K. Gupta, Imran Ali, Tawfik A. Saleh, Arunima Nayak, Shilpi Agarwal, RSC Advances 2 (2012) 6380–6388.
[49] V.K. Gupta, Alok Mittal, Jyoti Mittal, J. Colloid Interface Sci. 344 (2010) 497–507.
[50] V.K. Gupta, R. Jain, Shilpi Agarwal, M. Shrivastava, Mater. Sci. Eng.: C 31 (2011) 1062–1067.
[51] V.K. Gupta, Arunima Nayak, Chem. Eng. J. 180 (2012) 81–90.
[52] T.A. Saleh, V.K. Gupta, J. Colloids Interface Sci. 371 (2012) 101–106.
[53] H. Khani, M.K. Rofouei, P. Arab, V.K. Gupta, Z. Vafaei, J. Hazard. Mater. 183 (2010) 402–409.
[54] R. Jain, V.K. Gupta, N. Jadon, K. Radhapyari, Anal. Biochem. 407 (2010) 79–88.